Lab on a Chip

Micro- & nano- fluidic research for chemistry, physics, biology, & bioengineering

www.rsc.org/loc

Volume 10 | Number 22 | 21 November 2010 | Pages 2997–3184

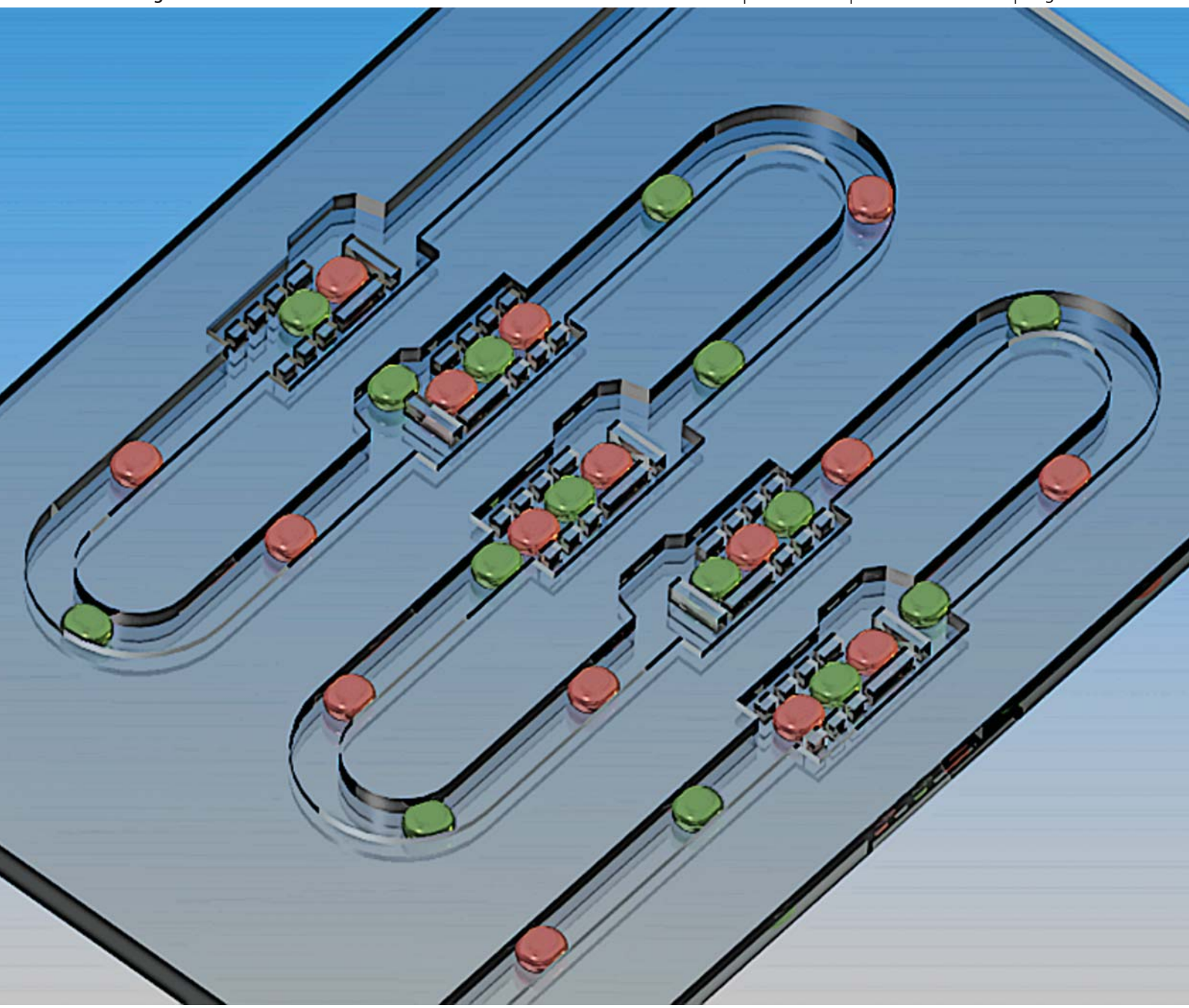

ISSN 1473-0197

RSC Publishing

PAPER
Zagnoni and Cooper
A microdroplet-based shift register

A microdroplet-based shift register†

Michele Zagnoni and Jonathan M. Cooper

Received 21st July 2010, Accepted 26th August 2010
DOI: 10.1039/c0lc00219d

A microfluidic device is presented for the serial formation, storage and retrieval of water microdroplets in oil. The principle of operation is similar to that of an electronic shift register. Droplets, considered as units of information, can be arrayed and serially shifted within the device, allowing the controllable positioning of the emulsions and the creation of interfaces between drops. Using this passive system, by exploiting the balance between hydrodynamic pressure and surface tension across a drop due to the device design, droplet networks can be readily arrayed in a series of elements and cascaded within the microchannels in an automatable and high throughput fashion. The results showed the suitability of the system to be used for the formation of artificial lipid bilayers and for the study of biological dynamic processes based on the diffusion of molecules through interfaces.

Introduction

The ability to control the flow behaviour at low Reynolds numbers, using passive microfluidic systems, is of fundamental importance to develop lab-on-a-chip (LOC) platforms characterised by enhanced functionalities with a minimum level of complexity. In particular, droplet-based microfluidics,[1,2] which can be employed to generate surfactant-stabilised liquid compartments using immiscible fluids, offer an additional advantage. By controlling the transport behaviour of water in oil (W/O) droplets within confined geometries, encapsulated particles or reagents can also be strategically positioned inside the microchannels. This feature has been previously used in two-phase microfluidic systems, proving successful either to trap microdroplets containing biological samples,[3,4] to study the diffusion behaviour of reagents across an interface between two droplets,[5] or to create artificial cell membranes. When two or more aqueous drops, submerged in a surfactant–solvent mixture, are brought together, two lipid monolayers self-assemble at each water–oil interface and form what is known as a droplet interface bilayer (DIB).[6] In recent years, several techniques to create stable DIBs have been proposed, where droplets were strategically positioned using either micromanipulators,[7] dielectrophoresis,[8] gravity[9] or, more recently, a high throughput setup that comprised syringe pumps and an autosampler to create DIBs stacked in three dimensions, inside polytetrafluoroethylene (PTFE) tubings.[10]

The prospect of integrating these functionalities together (*i.e.* to controllably position biological samples and to address molecular transport across interfaces), in a single automatable architecture, has significant future potential in LOC applications for the study of biological dynamic processes.

Here, we describe a system that enables the formation of combinatorial droplet-based networks in an automated and high throughput fashion with potential applications in the field of single-cell analysis (*i.e.* cells encapsulated in drops), artificial lipid bilayers (*i.e.* membrane protein characterisation) and in the study of transport of molecules across interfaces (*i.e.* drug diffusion to biological samples across membranes). The architecture not only enables the desired positioning of microdroplets, but also allows the formation of networks of interfaces, which can be used to control the selective transport of molecules between droplets, depending upon the type of surfactants employed.[5]

The device operation principle was inspired by that of electronic serial shift registers. Electronic shift registers are circuit elements used for a variety of time-delay and information storage applications.[11] A shift register is a form of memory consisting of components connected in a line, where the input data (unit of information) are sequentially stored and cascaded within the register for a predefined number of positions and synchronised by a clock pulse. Translating this electronic scheme into two-phase microfluidics, we built an equivalent droplet-based shift register, where each W/O droplet and its content represented a unit of information.

In this paper, we describe the characteristics and the functionalities of the architecture. The design of the device geometry provides an effective way to trap and maintain drops in a desired sequence (arrayed droplet networks) and enables the serial release of droplets from the network without loss of information. This approach could, in future, be used in LOC applications for the time control of diffusion of substances across membrane interfaces and for the specific recovery of droplets from the device for further processing of its content.

Experimental

W/O droplets were formed using the microfluidic geometry shown in Fig. 1a. A double T-junction was used to alternate two W/O droplet populations in a channel, forming "ABAB" array configurations. A commercially available pressure controller (MFCS 4C, Fluigent) was used to drive independently the phases into the device, applying pressure patterns typically in the range

School of Engineering, University of Glasgow, Glasgow, UK. E-mail: jmcooper@elec.gla.ac.uk; m.zagnoni@elec.gla.ac.uk; Fax: +44 (0)131 330 4907; Tel: +44 (0)131 330 4931

† Electronic supplementary information (ESI) available: Microfluidic device fabrication details; Movies S1, S2, S3, S4 and S5 show device operation, filling, storing, restarting and resetting functionalities. See DOI: 10.1039/c0lc00219d

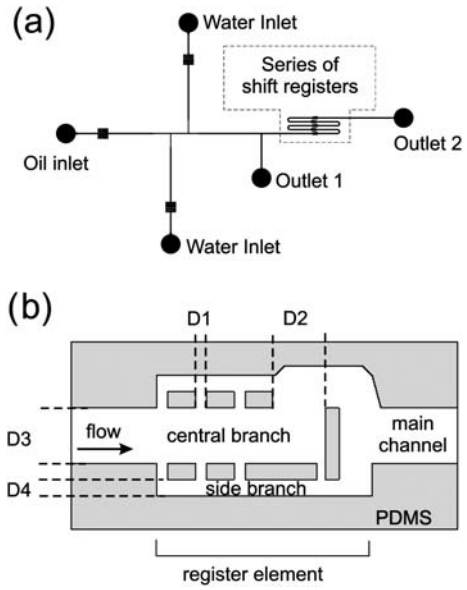

Fig. 1 Device geometry. (a) A double T-junction was used to generate W/O droplets. Outlet 1, between the junctions and the registers, was used during setup to extract residual air when filling the device and it was not used during normal device operation. A series of shift register elements of different lengths were used to create and store arrays of droplets. (b) The shift register element consisted of three channels (a central branch and two side branches) separated by rectangular pillars. The layout was designed to force the dispersed phase through the central branch, while the continuous phase mainly flowed in the two side branches. $D1 = 20$ μm, $D2 = 65$ μm, $D3 = 100$ μm, and $D4 = 30$ μm. Channel depth is 40 μm.

from 0 to 200 Pa. The system allowed the precise generation of on-demand droplet trains, thus enabling to start and stop drop formation in both junctions by adjusting, simultaneously, the pressure of the phases.

The microfluidic device was fabricated in polydimethylsiloxane (PDMS, Sylgard 184, Dow Corning) using standard photolithography methods (see fabrication details in ESI†). PDMS microchannels were irreversibly bonded to microscope glass slides using oxygen plasma. The microchannels were then treated with undiluted Aquapel (PPG Industries) to obtain fluorophilic surfaces and used with FC-40 (3M) fluorinated oil and 2 wt% EA surfactants (RainDance Technologies, Inc). Alternatively, for the formation of DIBs, the channels were treated with undiluted Sigmacote (Sigma Aldrich) and used with hexadecane (Sigma Aldrich) and either L-α-phosphatidylcholine (Soy-20%) or 1,2-dioleoyl-*sn-glycero*-3-phosphocholine (DOPC) lipids at 10 mg ml^{-1} (Avanti Polar Lipids).

In both cases, outlet 1 (Fig. 1a) was connected to a manually controlled valve. The valve was initially left in the open position, thus diverting the phases into waste until all the air was purged from the channels. The valve was then closed and outlet 1 was not used during normal device operation, where the droplets passed instead through a series of shift registers (highlighted by a dashed line in Fig. 1a) before exiting the chip. Devices were placed over an inverted microscope and imaging was acquired using a Labview controlled camera (EC 1280, Prosilica). ImageJ was used to analyse and process recorded images.

Fig. 1b shows the geometry of a shift register element. Within each register, the channel was designed to be wider than the main channel carrying the droplets and rectangular pillars were placed to create alternative fluidic pathways (a central branch and two side branches as shown in Fig. 1b), to influence the preferential flow of the phases. The distance between the pillars, $D1$, was designed to be smaller than that of the main channel, $D3$, in order to avoid droplets either to enter or to split into the side branches. Therefore, whilst the dispersed phase only followed the fluidic path constituted by the central branch of the register element, the continuous phase mainly flowed along the alternative paths in the two side branches.

Analogous element configurations have been previously reported, using PDMS pillars in microchannels to alter the fluid flow pathway. As examples, these have been used either to fuse W/O droplets[12] or for continuous sorting of mixed-sized particles.[13]

Results and discussion

A schematic sequence of the device operation is illustrated in Fig. 2a. After initial filling of the device with an oil phase, droplets that were at least 100 μm in diameter were generated by the two T-junctions (typical values were $P_{oil} = 100$ Pa, $P_{water1} = 80$ Pa, and $P_{water2} = 80$ Pa). When droplets reached an empty register, they remained trapped within the element, until they filled its entire length (Fig. 2a-1–3). Once this condition was reached, a new incoming droplet (upstream side in Fig. 2a-4) forced the drop at the end of the register to exit the element (downstream side in Fig. 2a-4), following a first-in-first-out (FIFO) pattern, and creating a serial shift of drops stored within the pillars. During each shift, the interfaces between drops remained stable and coalescence never occurred. When drop generation was stopped (whilst the oil phase was left to flow), droplets were successfully stored in the register (Fig. 2a-5). Fig. 2b shows a view of the device during operation (see also Movie S1 in ESI†) in which droplets were arrayed in ABAB configurations in a series of shift registers of different lengths. The number of droplets stored in a register element depended upon the drop size, as shown in Fig. 2c–e. Droplets with smaller dimension than the channel width (drop diameter < 70 μm) were not trapped within the element and kept flowing in the main channel after the register.

The operation principle of the device is based on the balance between hydrodynamic forces and surface tension forces due to the geometry of the register element, similarly to what has been previously proposed by Niu *et al.*[12] In microfluidic systems at low Reynolds numbers, the fluidic resistance, R, between two points in a rectangular channel can be described by the Hagen–Poiseuille relation. This quantifies R as the ratio of the pressure difference, ΔP, between these two points and the volumetric flow rate of a single fluid phase, Q, as:

$$R = \frac{\Delta P}{Q} = \frac{a\eta L}{WH^3}, \quad (1)$$

where η is the fluid viscosity, L the channel length, W the channel width, H the channel depth and a is a dimensionless parameter that depends upon the channel aspect ratio.[14,15]

When a droplet entered into an empty register element, it flowed to the downstream side of the central branch, following the path of lowest fluidic resistance (as the cross-section of the central branch is larger than that of the side branches). If the diameter of the droplet was larger than the width of the central

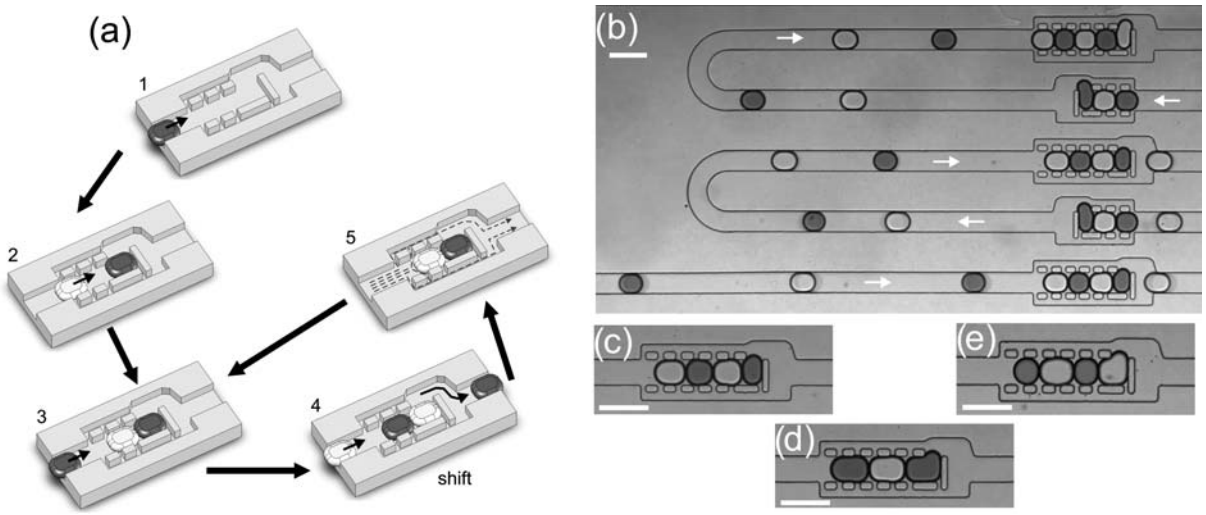

Fig. 2 Device operation. (a) Schematic sequence illustrating the working principle of a microfluidic shift register. After a register element was filled with the continuous phase, droplets arriving at the element were successfully trapped along its length in the central branch (a1–3). Any additional droplet arriving at the upstream side of the element forced the drop at the downstream side to exit the register (a4), creating a serial shift of the drops stored within the pillars. By controlling the pressure applied to the phases, droplet generation could be temporarily stopped to store droplets in the register. Dashed lines (a5) indicate the continuous phase flow lines during drop storage. (b) Image showing the operation of a series of shift registers of different lengths, where droplets were arrayed in "ABAB" configuration. (c–e) Images showing arrays of droplet networks stored in a register element having different drop sizes. Phases were FC40 with 2 wt% EA surfactants and Milli-Q water with food dye. Scale bars are 200 μm.

branch aperture ($D2$ in Fig. 1b), surface tension kept the droplet trapped between the pillars, whilst the oil phase continued to flow downstream both through the side branches and also through the gutters formed between the drop and the corners of the channel. Once a drop was trapped, the resistance of the channel changed, increasing considerably due to the decrease of the channel cross-section in the central branch (according to eqn (1)). A representation of a droplet-based shift register with an equivalent electric circuit is given in Fig. 3a, where the resistance of a register element can be approximately described by a distribution of constant and variable electric resistors.

As the system is driven by a constant pressure, the total flow rate will vary accordingly to the change in the fluid resistance, which depends upon the number of droplets trapped in the register. A simplified model of a register element is shown in Fig. 3b, where V_{CC} represents a constant pressure applied to the phases; R_1 represents the equivalent fluidic resistance of the channels from the pressure source to the point P_1; R_3 represents the equivalent fluidic resistance of the channels from the point P_2 to the outlet of the device; R_2 represents the fluidic resistance of the side branches and R_V represents the variable resistance of the central branch, due to the presence of one or more droplets. V_V is the potential drop across R_V and represents the differential pressure across a droplet when this is trapped inside the register. I_1, I_2, I_3 and I_V are the currents in each branch and represent the flow rates, respectively (where $I_1 = I_3 = I_2 + I_V$). The following expression can be obtained from the balance of the currents at the nodes of the circuit:

$$V_V = \frac{R_2 R_V}{R_V(R_1 + R_2 + R_3) + R_2(R_1 + R_3)} V_{CC}. \qquad (2)$$

V_V (eqn (2)) is a monotonic function which increases for increasing values of R_V. Thus, for a fixed V_{CC}, if R_V increases due to a droplet being trapped within the register, according to eqn (1), the differential pressure across such droplet can only increase and the magnitude and trend of the pressure jump will depend on the values of the resistors in the circuit.

Using this device design, every time a drop was trapped in the central channel, an increase in the differential pressure between the upstream (P_1, at the point x) and the downstream side (P_2, at the point y) of the drop was always obtained. This pressure increase acted to deform the drop and to push it through the

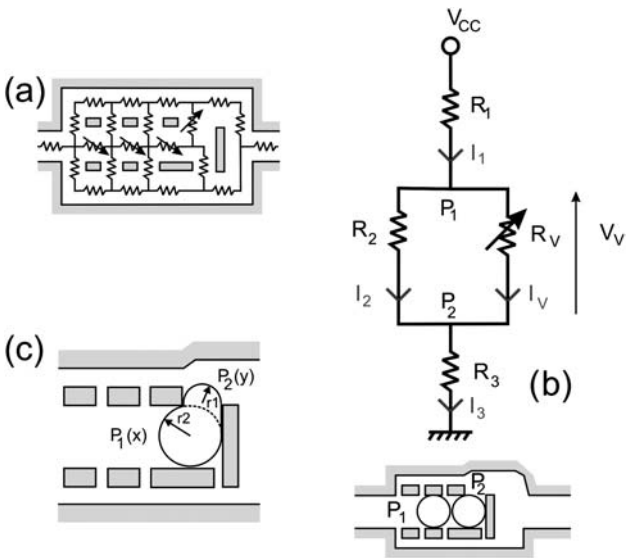

Fig. 3 (a) Equivalent electric model of a register element, where the channel network is represented with distributed electric resistors. (b) Simplified model of a register element using an equivalent electric circuit. (c) Schematic representation of the pressure balance between hydrodynamic and surface tension contribution across a trapped droplet within the register element.

aperture of the central branch (of width $D2$). As a response, surface tension forces in the droplet reacted against the hydrodynamic forces. According to the Laplace's law, the differential pressure between the inside and the outside of the droplet at the point x is given by $\Delta P_{back} = \gamma(1/r_2 + 2/H)$, whilst at the point y $\Delta P_{front} = \gamma(1/r_1 + 2/H)$, as shown schematically in Fig. 3c. Therefore, the droplet remained stored within the register element depending upon the balance of differential pressure between the points x and y, due to hydrodynamic pressure and surface tension, as formulated below:

$$P_1 - P_2 \leq \Delta P_{back} - \Delta P_{front} = -\gamma\left(\frac{1}{r_2} - \frac{1}{r_1}\right), \qquad (3)$$

where $r_1 = D2/2$. Typical values of the estimated differential pressure due to surface tension vary between 50 and 90 Pa. It can be noticed that the term at the right hand side of eqn (3) is independent of hydrodynamic parameters. Therefore, for a given geometry and condition of the phases, drop trapping should always be possible, providing that the flow can be stably controlled using very low pressure sources to reduce the hydrodynamic differential pressure ($P_1 - P_2$).

In a two-phase flow, hydrodynamic pressure is strongly influenced both by the number and the size of the droplets flowing in the channels and by the parameters of the phases,[14,16,17] therefore the velocity of the flow will be influenced also by the number of drops simultaneously flowing inside the channels. In addition, the operation principle discussed above can be applied also when more than one droplet is present in the register. As long as the differential pressure balance between the upstream side of the upstream drop and the downstream side of the downstream drop in each array was dominated by surface tension, droplets could be stably stored in the arrayed network within the register elements. When this condition was not satisfied or the register element was completely filled with drops throughout its length, the arrival of an additional droplet would create an increase in differential pressure across the whole array which overcame surface tension. In this case, the downstream drop in the element was deformed and dragged out in the main channel through the topside branch, re-establishing the previous condition of equilibrium. Using this design and selecting surfactant concentrations well above the critical micellar concentration (CMC), droplet splitting or coalescence never occurred, thus preserving the unit of information stored inside the drop.

Several functionalities were reliably obtained by controlling the pressure values applied to the phases, as shown in Fig. 4a–d. After filling the register with a predefined drop size (Fig. 4a and Movie S2 in ESI†), droplets could be stored within the element by suddenly reducing the pressure applied to the water phases (typically from 80 Pa to 20 Pa) and to the oil phase (typically from 100 Pa to 60 Pa). Drops could remain stored in the registers until the oil phase supply was depleted (Fig. 4b and Movie S3 in ESI†). After a storage condition was achieved, droplet generation could be restarted by restoring the original pressure conditions of the phases (Fig. 4c and Movie S4 in ESI†). Finally, a reset function could also be obtained. By increasing temporarily the pressure applied to one of the water phases ($P_{water} > P_{oil}$ in a step-like manner), a long W/O droplet (or "slug") could be produced. This, being longer than the length of the registers, produced a differential hydrodynamic pressure across the element that was always able to sequentially empty all the registers, dragging out previously trapped droplets. Once this was achieved, a new filling procedure could be initiated (Fig. 4d and Movie S5 in ESI†).

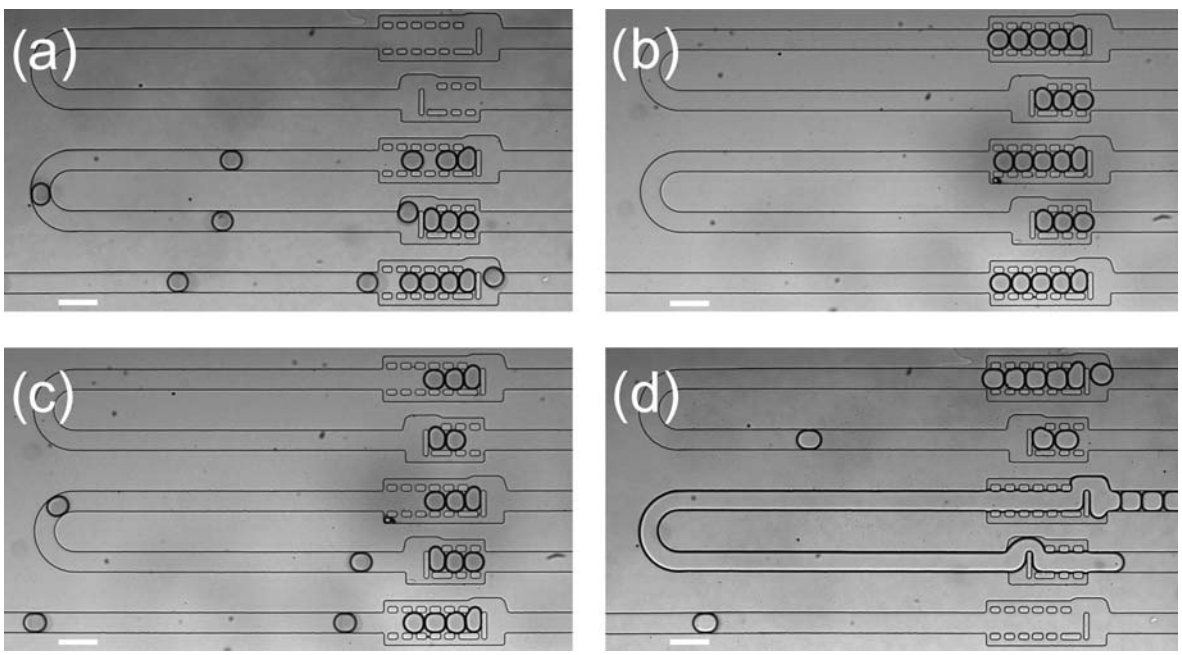

Fig. 4 Functionalities obtained using a droplet-based shift register. (a) Empty registers were initially filled with droplets (Movie S2 in ESI†). (b) Droplets were stored within the registers (Movie S3 in ESI†). (c) Droplet generation restarted after storage (Movie S4 in ESI†). (d) A drop (or "slug") longer than the length of a single register element was generated to reset all the elements (Movie S5 in ESI†) and filling subsequently restarted. Phases were FC40 with 2% EA surfactants and Milli-Q water with food dye. Scale bars are 200 μm.

Once droplets were stably stored in the device, the pressure applied to the oil phase could be decreased and subsequently increased, within a range of pressure values that maintained the drops trapped. As shown in Fig. 5a, this produced a clear reversible deformation of the drops arrayed within the registers and induced the interfaces of contact to vary their length by approximately 20% for a difference in oil pressure of 20 Pa. As molecular diffusion across an interface is related to its area, having control over the drop deformation could be a useful parameter to obtain dynamic control over a diffusion process across an interface between droplets.

Finally, the system was tested using hexadecane and biologically relevant phospholipids to investigate the performance of the shift register design to create artificial lipid bilayers. Organic solvents are well known to be absorbed by PDMS,[18,19] thus creating swelling of the features in the microchannels. This represented a major problem in our PDMS architecture, as the behaviour of the register was strongly influenced by the value of the fluidic resistance of the channels. Nevertheless, although the register element geometry was altered, droplet interface bilayers could still be formed by adjusting the pressure sources to accommodate the new hydrodynamic and surface tension conditions, as previously discussed.

Results are shown in Fig. 5b. Although the gaps between the pillars of the PDMS shift register were noticeably reduced due to solvent uptake and swelling (40% with respect to the case of fluorinated oil, as seen from the comparison between the two cases in Fig. 5), droplets could still be arrayed and stored within the register elements using lower pressure values applied to the phases (typically $P_{oil} = 55$ Pa, $P_{water1} = 40$ Pa and $P_{water2} = 40$ Pa). This preliminary result provides an alternative technique to create DIBs to those already presented[8,10] and opens the way to the development of high throughput microfluidic platforms to create arrayed networks of DIBs. These characteristics can play a fundamental role in the automation of systems to be used in the fields of bilayer lipid membrane related research, providing a possible solution to eliminate manual intervention.

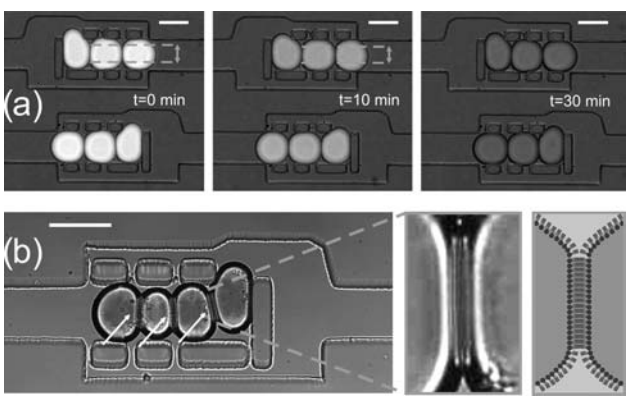

Fig. 5 (a) Temporal sequence of fluorescence microscopy images showing droplet storage within the registers. Phases were FC40 with 2% EA surfactants and Milli-Q water with 250 μM fluorescein. Light source excitation was always left on during recording. At $t = 0$ and $t = 30$ min, the pressure applied to the continuous phase ($P_{oil} = 60$ Pa) was higher than at $t = 10$ min ($P_{oil} = 40$ Pa). For a lower applied pressure, droplets are noticeably less deformed. Dashed lines indicate the length of the interface between drops. Scale bar is 100 μm. (b) Droplet storage within a register, forming a network of droplet interface bilayers (DIBs). Phases were hexadecane with DOPC lipids at 10 mg ml^{-1} and 100 mM KCl. Arrows indicate DIBs. On the right: a close-up image and a schematic representation of a DIB, respectively.

Conclusions

In this paper, we have described the operation of a microfluidic droplet-based shift register. This architecture enables new functionalities to be achieved in an automatable and high throughput manner, including the formation of combinatorial droplet-based sequences and droplet retrieval, exploiting the serial working properties of the system. We anticipate our intention to integrate polymeric valves in the current architecture to better address on-demand droplet formation,[20,21] thus enhancing the combinatorial capability of the system, and to develop the shift register structure using solvent resistant materials (*i.e.* poly(methyl methacrylate) and glass). The implementation of these features in the system has significant future potential to develop applications in the fields of dynamic biological processes based on molecular diffusion across interfaces and also in drug screening using automatable DIB systems.

Acknowledgements

This work was supported by BBSRC (BB/F005024/1).

References

1 S. Teh, R. Lin, L. Hung and A. P. Lee, *Lab Chip*, 2008, **8**, 198–220.
2 G. F. Christopher and S. L. Anna, *J. Phys. D: Appl. Phys.*, 2007, **40**, R318–R336.
3 W. Shi, J. Qin, N. Ye and B. Lin, *Lab Chip*, 2008, **8**, 1432–1435.
4 C. H. J. Schmitz, A. C. Rowat, S. Koster and D. A. Weitz, *Lab Chip*, 2009, **9**, 44–49.
5 Y. Bai, X. He, D. Liu, S. N. Patil, D. Bratton, A. Huebner, F. Hollfelder, C. Abell and W. T. S. Huck, *Lab Chip*, 2010, **10**, 1281–1285.
6 M. A. Holden, D. Needham and H. Bayley, *J. Am. Chem. Soc.*, 2007, **129**, 8650–8655.
7 G. Maglia, A. J. Heron, W. L. Hwang, M. A. Holden, E. Mikhailova, Q. Li, S. Cheley and H. Bayley, *Nat. Nanotechnol.*, 2008, **4**, 347–440.
8 S. Aghdaei, M. E. Sandison, M. Zagnoni, N. G. Green and H. Morgan, *Lab Chip*, 2008, **8**, 1617–1620.
9 M. Zagnoni, M. E. Sandison, P. Marius and H. Morgan, *Anal. Bioanal. Chem.*, 2009, **393**, 1601–1605.
10 C. E. Stanley, K. S. Elvira, X. Z. Niu, A. D. Gee, O. Ces, J. B. Edel and A. J. deMello, *Chem. Commun.*, 2010, **46**, 1620–1622.
11 V. P. Nelson, H. Troy Nagle, B. D. Carroll and D. Irwin, *Digital Logic Circuit Analysis and Design*, Prentice Hall, 1995.
12 X. Niu, S. Gulati, J. B. Edel and A. J. deMello, *Lab Chip*, 2008, **8**, 1837–1841.
13 P. B. Lillehoj, H. Tsutsui, B. Valamehr, H. Wub and C. Ho, *Lab Chip*, 2010, **10**, 1678–1682.
14 M. J. Fuerstman, A. Lai, M. E. Thurlow, S. S. Shevkoplyas, H. A. Stone and G. M. Whitesides, *Lab Chip*, 2007, **7**, 1479–1489.
15 C. J. Morris and F. K. Forster, *Exp. Fluids*, 2004, **36**, 928–937.
16 B. J. Adzima and S. S. Velankar, *J. Micromech. Microeng.*, 2006, **16**, 1504–1510.
17 S. A. Vanapalli, A. G. Banpurkar, D. van den Ende, M. H. G. Duits and F. Mugele, *Lab Chip*, 2009, **9**, 982–990.
18 J. Ng Lee, C. Park and G. M. Whitesides, *Anal. Chem.*, 2003, **75**, 6544–6554.
19 N. Malmstadt, M. A. Nash, R. F. Purnell and J. J. Schmidt, *Nano Lett.*, 2006, **6**, 1961–1965.
20 J. Galas, D. Bartolo and V. Studer, *New J. Phys.*, 2009, **11**, 075027.
21 S. Zeng, B. Li, X. Su, J. Qin and B. Lin, *Lab Chip*, 2009, **9**, 1340–1343.